Interferometric description of optical nanomaterials

P. Grahn, A. Shevchenko, and M. Kaivola
Department of Applied Physics, Aalto University, P.O. Box 13500, FI-00076 Aalto, Finland
(Dated: March 27, 2013)

We introduce a simple analytical model that describes the interaction of light with optical nanomaterials in terms of interfering optical plane waves. In this model, a nanomaterial is considered to consist of planar arrays of nanoparticles. In the analysis, each such array reduces to a thin homogeneous sheet that has one transmission and in general two reflection coefficients. These coefficients are found to be equal to those of an isolated planar array of the nanoparticles. The presented theory enables fast analytical calculation of the light transmission and reflection by nanomaterial slabs of arbitrary sizes. It is also shown to accurately describe optically anisotropic nanomaterials that in addition exhibit strong spatial dispersion, such as bifacial nanomaterials.

Optical nanomaterials are man-made materials composed of densely packed subwavelength-size nanoparticles appearing like artificial atoms to light. While the optical response of each individual nanoparticle can be revealed using, e.g., the electromagnetic multipole expansion[1], the description of the macroscopic optical response of a real three-dimensional nanomaterial still remains a challenge. This description is complicated by non-trivial interactions between the nanoparticles, including evanescent-wave coupling between them. In this work, we however propose a way to calculate the transmission and reflection characteristics of essentially arbitrary nanomaterial slabs, including anisotropic and spatially dispersive ones, without resorting to evanescent waves.

So far, both numerical[2–5] and experimental[6–8] techniques have been used to obtain the transmission and reflection coefficients for nanomaterial slabs with a rather limited number of nanostructured layers. The coefficients obtained for such slabs do not accurately describe the properties of a bulk nanomaterial. One approach to extract the bulk properties would be to successively increase the number of layers and see if the optical characteristics converge[2–4]. However, the understanding of the real physics that determines the final transmission properties is lost when using this procedure. In the description proposed in this work, the properties of a bulk nanomaterial slab are directly linked to the properties of a single layer of the material.

Recently, in connection with metamaterials, several retrieval procedures have been introduced to obtain effective wave parameters, such as electric permittivity and magnetic permeability, from the reflection and transmission coefficients of a nanomaterial slab[9,10]. These retrieval procedures rely upon the Fresnel coefficients which are derived for dipolar media. However, for the class of bifacial nanomaterials in which the electric quadrupole excitations are present[11], the classical electromagnetic boundary conditions do not hold[12,13]. Consequently, neither the Fresnel coefficients nor the retrieval procedures can be applied to these nanomaterials. The development of an adequate theory for the description of highly spatially dispersive nanomaterials, such as bifacial nanomaterials, would be of great practical importance, e.g., for solar cell applications.

In this work, we re-examine the propagation of light through an arbitrary slab of bifacial optical nanomaterial. We find that both the transmission and reflection by the slab can be surprisingly accurately described in terms of propagating optical plane waves only, which dramatically simplifies the description. Using rigorous numerical calculations we verify the accuracy of our approach and find that in many cases, the role of the evanescent waves for the energy transfer between adjacent nanomaterial layers can indeed be neglected.

Consider a nanomaterial slab that is created by stacking two-dimensional arrays of nanoscatterers in a transparent dielectric medium (see Fig. 1a). When illuminated by an optical plane wave, the first layer of nanoscatterers transmits a certain portion of the incident field. A part of this transmitted field is then reflected back by the second layer and the rest is partially absorbed and partially transmitted further to the third layer. Provided that the nanomaterial periodicity is much smaller than the illumination wavelength, no diffracted orders will occur and the propagating field between the neighboring layers will consist of two optical plane waves. Neglecting possible evanescent-wave couplings between the layers, we describe each layer as an infinitesimally thin sheet surrounded by the host dielectric (see Fig. 1b). The total transmission and reflection of the slab is then described in terms of the transmission and reflection coefficients of the individual sheets in a way resembling the description of Fabry-Perot interferometers.

Our approach is as follows. For a single isolated layer of a nanomaterial, we first numerically calculate the transmission and reflection coefficients and assign them to an equivalent infinitesimally thin sheet in the middle of the unit cells. These coefficients depend on both the angle of incidence θ and the polarization of the incident field. In addition, for bifacial nanoscatterer arrays, the reflection coefficient changes if the illumination direction is reversed[11,14]. Therefore, for the wave propagating to the right (left) within the nanomaterial, we use the reflection coefficient ρ_L (ρ_R) to describe the reflection from the left (right) side of each layer. Optical reciprocity ensures that the transmission coefficient τ must be the same for both waves. When calculated in this way, the parameters ρ_L, ρ_R and τ automatically include the near- and far-field

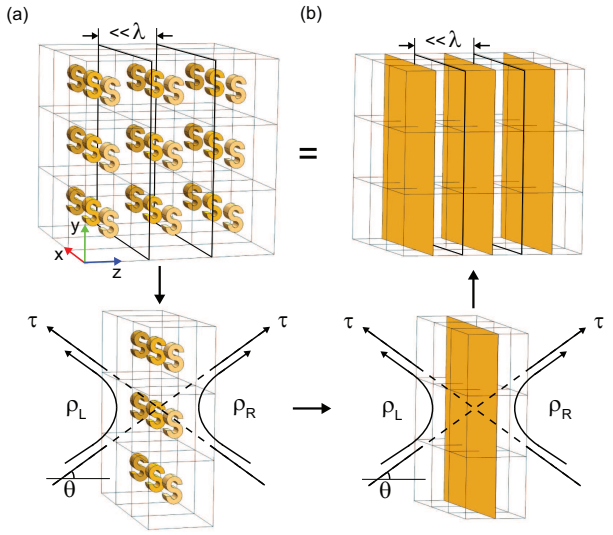

FIG. 1. A nanomaterial slab (a) that is composed by stacking layers of arbitrary scatterers, S, is described as (b) an array of infinitesimally thin sheets. The transmission and reflection coefficients (τ, ρ_L and ρ_R) for each of these sheets are taken to be equal to those of a single isolated layer of the nanomaterial.

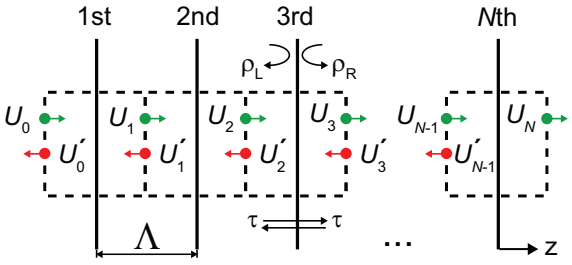

FIG. 2. Light propagation through a nanomaterial described by an array of infinitesimally thin sheets. Between each pair of such sheets there are two counter-propagating plane waves with transverse field components U_j and $U_j^{'}$. The unit cells of the nanomaterial are shown with dashed lines.

coupling between the scatterers within the layer in question. This coupling makes the extent of the evanescent wave along the layer's normal shorter for denser packing of the scatterers.

Let a plane wave with a transverse field amplitude U_0 and a wave vector $\boldsymbol{k}_{\rm in} = \hat{\boldsymbol{x}}k_x + \hat{\boldsymbol{z}}k_z$ be incident on a nanomaterial slab that consists of N layers of thickness Λ and has its surface normal along the z axis (see Fig. 2). The wave can be either TE- or TM-polarized. Treating each nanoscatterer layer as an infinitesimally thin sheet, we consider the counter-propagating waves between the sheets to have wave vectors $\boldsymbol{k}_{\pm} = \hat{\boldsymbol{x}}k_x \pm \hat{\boldsymbol{z}}k_z$, because the material between the sheets is considered to be the same as outside the slab. The transverse fields U_j and $U_j^{'}$ after each sheet j in Fig. 2 must satisfy the following equations

$$U_j = fU_{j-1} + g_R U_j^{'}, \tag{1}$$

$$U_j^{'} = g_L U_j + fU_{j+1}^{'}, \tag{2}$$

where $f = \tau\exp(ik_z\Lambda)$, $g_L = \rho_L\exp(ik_z\Lambda)$ and $g_R = \rho_R\exp(ik_z\Lambda)$. Using Eqs. (1) and (2), we derive separate relations for the forward and backward propagating fields

$$U_{j+1} + U_{j-1} - \alpha U_j = 0, \tag{3}$$

$$U_{j+1}^{'} + U_{j-1}^{'} - \alpha U_j^{'} = 0, \tag{4}$$

where $\alpha = f + f^{-1}(1 - g_L g_R)$. With the help of Eqs. (1) and (3) and the fact that $U_N^{'} = 0$, we obtain the transmission coefficient of the slab to be

$$t = \frac{U_N}{U_0} = \frac{f}{G_N(\alpha) - fG_{N-1}(\alpha)}. \tag{5}$$

Here we have introduced the G-polynomial that is calculated as

$$G_0(\alpha) = 0, \tag{6}$$

$$G_1(\alpha) = 1, \tag{7}$$

$$G_j(\alpha) = \alpha G_{j-1}(\alpha) - G_{j-2}(\alpha). \tag{8}$$

Similarly, using Eqs. (1), (2) and (4) we derive the reflection coefficient

$$r = \frac{U_0^{'}}{U_0} = g_L G_N(\alpha) f^{-1} t. \tag{9}$$

Equations (5) and (9) enable direct calculation of the transmission and reflection coefficients of an arbitrarily thick nanomaterial in terms of the transmission and reflection coefficients of an *isolated* monolayer of the nanomaterial. For $N = 1$, Eqs. (5) and (9) correctly yield $t = \tau\exp(ik_z\Lambda)$ and $r = \rho_L\exp(ik_z\Lambda)$ and for $N = 2$ the well-known results for a Fabry-Perot etalon are obtained.

In order to demonstrate the applicability of our theory, we compare it with rigorous numerical calculations. This is done by selecting some non-trivial nanoscatterers, such as nanoshells (Fig. 3a), nanorings (Fig. 4a) and nanodimers (Fig. 5a). These nanoscatterers are considered to compose stacks of two-dimensional periodic arrays that are embedded in a dielectric host medium of refractive index 1.5. The transmission and reflection coefficients for a single array are computed numerically using the computer software COMSOL Multiphysics. The obtained coefficients are then used in Eqs. (5) and (9) to acquire the transmission and reflection coefficients for several layers. These coefficients are compared with the results of direct numerical calculations of the whole stack with COMSOL. For these calculations we choose TM-polarized illumination with $\theta = 45^\circ$ and a slab consisting of $N = 5$ layers. This choice is general enough for demonstrating the applicability of the model.

We first consider a nanomaterial with an isotropic unit cell containing a silver nanoshell as depicted in Fig. 3a. The nanoshells have an outer radius $R = 35$ nm and a thickness $h = 7$ nm. They form a cubic lattice with period $\Lambda = 130$ nm. The optical properties of such

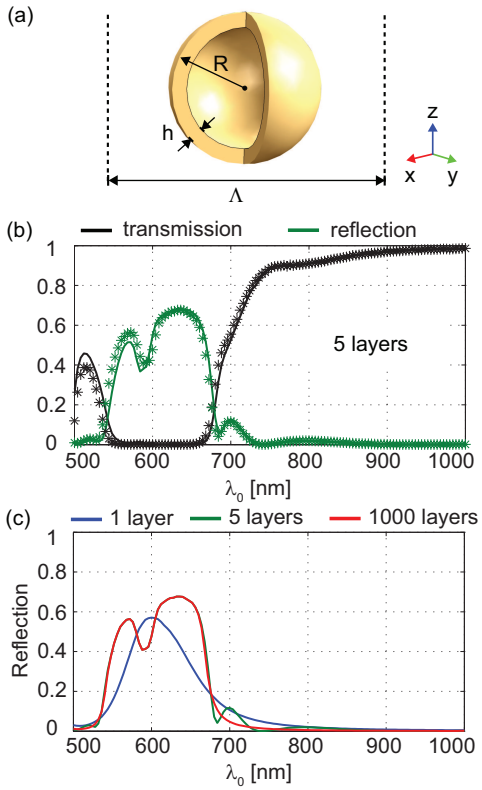

FIG. 3. (a) Geometry of the nanoshell [$R = 35$ nm, $h = 7$ nm, $\Lambda = 130$ nm]. (b) Transmission and reflection spectra of a five-layer thick slab for TM-polarized incident light with the angle of incidence of 45°. The numerically calculated spectra (solid lines) are shown along with the the analytical results (stars) obtained from Eqs. (5) and (9). (c) Reflection spectra for increasing number of layers as obtained from Eqs. (5) and (9).

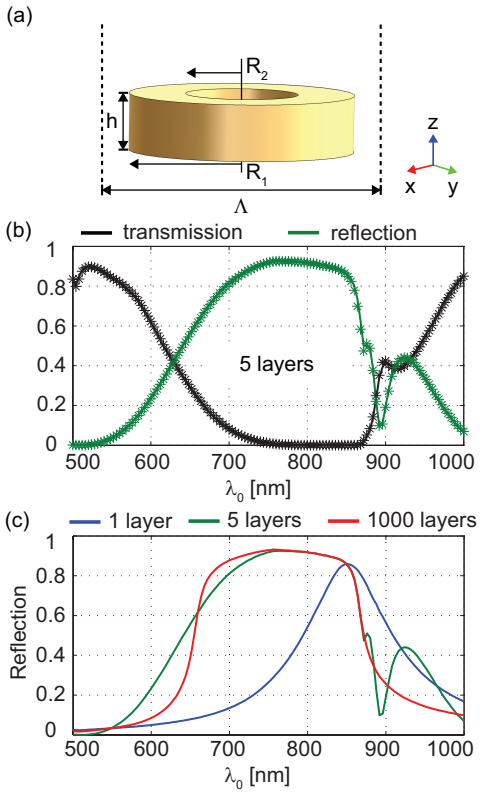

FIG. 4. (a) Geometry of the nanoring [$R_1 = 20$ nm, $R_2 = 10$ nm, $h = 10$ nm, $\Lambda = 50$ nm]. (b) and (c) are as in Fig. 3.

nanoshells are well investigated[15,16] and similar structures can be relatively readily fabricated[17,18]. For the calculations, the optical characteristics of silver were taken from Ref. 19. The calculated transmission and reflection spectra in the wavelength range from 500 to 1000 nm for the nanoshell slab are shown in Fig. 3b. The spectra obtained by using Eqs. (5) and (9) are in a good agreement with the direct numerical calculations, indicating that the plane-wave description of the light propagation is appropriate and that the evanescent-wave coupling between the layers is weak. While direct numerical calculations are always limited by the present computational resources, the introduced theory allows us to calculate the response of an arbitrarily thick slab. In Fig. 3c the reflection spectrum for a slab of 1000 nanoshell layers is shown by the red curve. For this particular case of nanoshells, the spectrum of 1000 layers is close to the spectrum of the 5-layer slab and it is already indistinguishable from the spectrum of an infinitely thick nanomaterial.

Next, we introduce an anisotropic (uniaxial) unit cell containing a silver nanoring as depicted in Fig. 4a. The ring has an outer radius $R_1 = 20$ nm, inner radius $R_2 = 10$ nm and thickness $h = 10$ nm. The rings form a cubic lattice with period $\Lambda = 50$ nm, such that each layer is aligned with the xy-plane. The calculated transmission and reflection spectra for the nanoring slab are shown in Fig. 4b. The theory yields excellent agreement with direct numerical calculations also for these nanoscatterers. The reflection for 1000 layers, depicted by the red curve in Fig. 4c, shows that the bulk nanomaterial behaves quite differently from a single layer due to the interlayer interaction. One can notice that if the number of layers is large, the nanomaterial acts as a spectrally selective broad-band reflector with a nearly flat-top spectral profile.

As a final example, we consider a bifacial nanomaterial slab that exhibits strong spatial dispersion. To our knowledge such nanomaterials have not been previously described in terms of their reflection and transmission characteristics. The unit cells of the material contain asymmetric silver nanodimers (see Fig. 5a). These nanodimers have been shown to exhibit complete suppression of the electric dipole excitation in a narrow wavelength range when illuminated from the smaller disc side[11]. However, in a nanomaterial, there will be two counter-propagating waves and the electric dipole moment cannot be suppressed for both of them simultaneously[14]. The nanodimer geometry is described by the radii $R_1 = 15$ nm and $R_2 = 20$ nm of the discs and dimensions $h = s =$

10 nm defined in Fig. 5a. A cubic lattice with period $\Lambda = 50$ nm is now composed of the nanodimers such that the smaller discs are on the left-hand side. As a consequence of the asymmetry of the unit cell, we calculate the single layer response to illumination from both sides in order to obtain the reflection coefficients ρ_L and ρ_R.

Using Eqs. (5) and (9) we calculate the transmission and reflection spectra for a nanodimer slab illuminated from the two sides and compare them with the numerical results. Figure 5b shows that while the theory very accurately resolves all spectral features, there is a slight deviation of the analytically obtained values from the exact numerical values for the wavelengths around 600 nm. This deviation obviously originates from the evanescent-wave coupling between the adjacent layers. However, considering that the gap size between the discs in the adjacent layers is only 20 nm, the agreement is still remarkably good. We obtained a similar good agreement between our theory and the numerical calculations also for angles of incidence of 0, 30 and 60 degrees as well as for the TE-polarization. The reflection spectra of 1000 layers of nanodimers are depicted in Fig. 5c. When illuminated from the small disc side, the reflection coefficient significantly decreases at around the electric dipole suppression wavelength of 618 nm.

The accuracy of the presented theory depends on the extent of the evanescent waves in the direction of light propagation. Qualitatively, for the theory to be exact, the evanescent waves associated with the cut-off diffraction orders must have a decay length that is much shorter than the spacing between the particles in two adjacent layers. For a two-dimensional square array of period $\Lambda_x = \Lambda_y$, the longitudinal wave vector of the first such order $k_{z1} = [k^2 - (2\pi/\Lambda_x - k_x)^2]^{1/2}$ is imaginary, with k and k_x being the magnitudes of the total and transverse wave numbers of the incident light. The next order would be $k_{z2} = [k^2 - (2\pi/\Lambda_x + k_x)^2]^{1/2}$. We define the decay length δ of the evanescent field to be the distance for which the field amplitude has decayed by a factor of $\exp(-1)$. The gap d between the particles in the z direction must then be much larger than

$$\delta = \frac{1}{\mathrm{Im}\{k_{z1}\}} = [(\frac{2\pi}{\Lambda_x} - k_x)^2 - k^2]^{-1/2}. \qquad (10)$$

Considering the nanoshells with $\Lambda_x = 130$ nm, $\lambda_0 = 500$ nm and $k_x = k/\sqrt{2}$, we obtain a decay length $\delta \approx 34$ nm that is smaller than the 60 nm gap between the adjacent shells. For the nanodimers, with $\Lambda_x = 50$ nm, $\lambda_0 = 500$ nm and $k_x = k/\sqrt{2}$, the decay length is $\delta \approx 9$ nm. This value is smaller than the gap $d = 20$ nm between the nanodimers, which supports the success of our analytical calculations. We note that for a nanomaterial to be homogenizable, it is required that $k << 2\pi/\Lambda_x$. Equation (10) then yields an evanescent wave decay length of $\Lambda_x/(2\pi)$ and the criterion for neglecting the evanescent-wave coupling becomes $d >> \Lambda_x/(2\pi)$. As a practical criterion for when our theory can be applied to a homogenizable nanomaterial, we require that $d > \Lambda_x/2$.

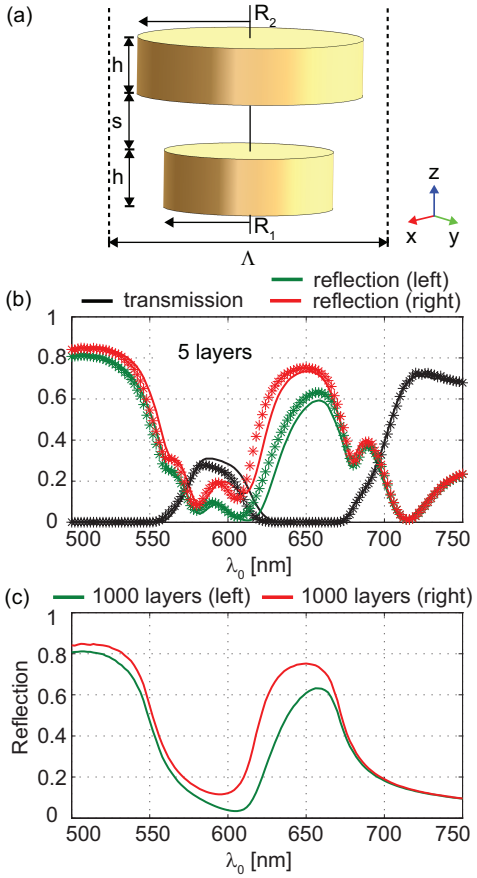

FIG. 5. (a) Geometry of the disc nanodimer [$R_1 = 15$ nm, $R_2 = 20$ nm, $h = s = 10$ nm, $\Lambda = 50$ nm]. (b) is as in Fig. 3b. The green (red) color corresponds to the illumination from the side of the smaller (larger) discs. (c) Reflection spectra for 1000 layers as obtained from Eqs. (5) and (9).

In order to verify the above predictions on the influence of the evanescent waves, we numerically calculate the transmission through the nanodimer slab, while varying the transverse and longitudinal periods separately. In Fig. 6a the transmission coefficient is plotted for an increasing longitudinal period Λ_z. The transverse period is fixed to $\Lambda_x = 100$ nm in order to have the evanescent-wave coupling significant enough to cause a discrepancy at small Λ_z between the theory and the numerical results. We notice that when d exceeds $\Lambda_x/2$ [Λ_z exceeds 80 nm], this discrepancy disappears. The transmission coefficient for an increasing transverse period $\Lambda_x = \Lambda_y$ is shown in Fig. 6b. In this case the longitudinal period is fixed to $\Lambda_z = 70$ nm, such that the evanescent-wave coupling is negligible at $\Lambda_x = 50$ nm. As the transverse period is increased, the discrepancy between the theory and the numerical results starts to appear due to an increase in the evanescent wave decay length. We notice however that as Λ_x is increased, the array also gets sparse, which reduces the influence of the nanoscatterers on the propagating wave. This effect counterbalances the growing

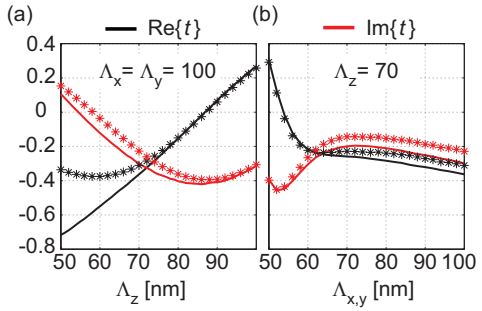

FIG. 6. Transmission coefficient t of a five-layer thick nanodimer slab for (a) increasing period Λ_z with fixed $\Lambda_x = \Lambda_y = 100$ nm and (b) increasing $\Lambda_x = \Lambda_y$ with fixed $\Lambda_z = 70$ nm. A TM-polarized illumination with $\lambda_0 = 600$ nm and $\theta = 45^\circ$ (from smaller disc side) is considered. The numerically calculated results (solid lines) are shown along with the analytical results (stars) obtained from Eqs. (5) and (9).

decay length of the evanescent waves such that the discrepancy between the theory and the numerical results remains small.

In summary, we have introduced a simple analytical theory for the description of light interaction with optical nanomaterials. Recognizing the subwavelength size of the nanomaterial's unit cells, we found that the evanescent-wave coupling between adjacent monolayers of the nanomaterial does not significantly influence the light propagation in the material. As a consequence, the nanomaterial can be accurately described in terms of the plane-wave transmission characteristics obtained for a single isolated monolayer. The presented numerical calculations demonstrate the wide applicability of this remarkably simple analytical model.

In contrast to existing theoretical approaches, our one also correctly describes three-dimensional arrays of bifacial nanoscatterers, which is of practical importance for a large variety of nanomaterials, such as metamaterials with asymmetric unit cells. For both symmetric and bifacial nanomaterial slabs, our method enables rapid extraction of the transmission and reflection coefficients, which can for example be used to calculate the effective wave parameters, such as ϵ and μ, via the known retrieval procedures[9,10]. Furthermore, propagation of optical beams through such nanomaterials can be described by using the angular spectrum representation with our model applied to each plane-wave component. We believe that the presented theory has the necessary simplicity and accuracy to accelerate the development of optical nanomaterials tailored for real applications.

ACKNOWLEDGMENTS

This work was funded by the Academy of Finland (Project No. 134029).

[1] P. Grahn, A. Shevchenko, and M. Kaivola, New Journal of Physics **14**, 093033 (2012).
[2] A. Andryieuski, C. Menzel, C. Rockstuhl, R. Malureanu, F. Lederer, and A. Lavrinenko, Phys. Rev. B **82**, 235107 (2010).
[3] R. Paniagua-Domínguez, F. López-Tejeira, R. Marqués, and J. A. Sánchez-Gil, New Journal of Physics **13**, 123017 (2011).
[4] W.-C. Chen, A. Totachawattana, K. Fan, J. L. Ponsetto, A. C. Strikwerda, X. Zhang, R. D. Averitt, and W. J. Padilla, Phys. Rev. B **85**, 035112 (2012).
[5] R. Alaee, C. Menzel, A. Banas, K. Banas, S. Xu, H. Chen, H. O. Moser, F. Lederer, and C. Rockstuhl, Phys. Rev. B **87**, 075110 (2013).
[6] E. Pshenay-Severin, F. Setzpfandt, C. Helgert, U. Hübner, C. Menzel, A. Chipouline, C. Rockstuhl, A. Tünnermann, F. Lederer, and T. Pertsch, J. Opt. Soc. Am. B **27**, 660 (2010).
[7] M. Choi, S. H. Lee, Y. Kim, S. B. Kang, J. Shin, M. H. Kwak, K.-Y. Kang, Y.-H. Lee, N. Park, and B. Min, Nature **470**, 369 (2011).
[8] B. Gompf, B. Krausz, B. Frank, and M. Dressel, Phys. Rev. B **86**, 075462 (2012).
[9] D. R. Smith, S. Schultz, P. Markoš, and C. M. Soukoulis, Phys. Rev. B **65**, 195104 (2002).
[10] C. Menzel, C. Rockstuhl, T. Paul, F. Lederer, and T. Pertsch, Phys. Rev. B **77**, 195328 (2008).
[11] P. Grahn, A. Shevchenko, and M. Kaivola, Phys. Rev. B **86**, 035419 (2012).
[12] E. B. Graham and R. E. Raab, Proc. R. Soc. Lond. A **456**, 1193 (2000).
[13] E. B. Graham and R. E. Raab, Proc. R. Soc. Lond. A **457**, 471 (2001).
[14] P. Grahn, A. Shevchenko, and M. Kaivola, Journal of the European Optical Society - Rapid publications **8**, 13009
[15] C. G. Khoury, S. J. Norton, and T. Vo-Dinh, Nanotechnology **21**, 315203 (2010).
[16] Y.-W. Ma, J. Zhang, L.-H. Zhang, G.-S. Jian, and S.-F. Wu, Plasmonics **6**, 705 (2011).
[17] K.-T. Yong, Y. Sahoo, M. T. Swihart, and P. N. Prasad, Colloids and Surfaces A: Physicochemical and Engineering Aspects **29**
[18] B. G. Prevo, S. A. Esakoff, A. Mikhailovsky, and J. A. Zasadzinski, Small **4**, 1183 (2008).
[19] P. B. Johnson and R. W. Christy, Phys. Rev. B **6**, 4370 (1972).